The NEW ENGLAND JOURNAL of MEDICINE

ESTABLISHED IN 1812 JUNE 13, 2024 VOL. 390 NO. 22

Risk of Second Tumors and T-Cell Lymphoma after CAR T-Cell Therapy

Mark P. Hamilton, M.D., Ph.D., Takeshi Sugio, M.D., Ph.D., Troy Noordenbos, M.D., Ph.D., Shuyu Shi, B.Med., Philip L. Bulterys, M.D., Ph.D., Chih Long Liu, Ph.D., Xiaoman Kang, B.S., Mari N. Olsen, B.S., Zinaida Good, Ph.D., Saurabh Dahiya, M.D., Matthew J. Frank, M.D., Ph.D., Bita Sahaf, Ph.D., Crystal L. Mackall, M.D., Dita Gratzinger, M.D., Ph.D., Maximilian Diehn, M.D., Ph.D., Ash A. Alizadeh, M.D., Ph.D., and David B. Miklos, M.D., Ph.D.

ABSTRACT

BACKGROUND

The risk of second tumors after chimeric antigen receptor (CAR) T-cell therapy, especially the risk of T-cell neoplasms related to viral vector integration, is an emerging concern.

METHODS

We reviewed our clinical experience with adoptive cellular CAR T-cell therapy at our institution since 2016 and ascertained the occurrence of second tumors. In one case of secondary T-cell lymphoma, a broad array of molecular, genetic, and cellular techniques were used to interrogate the tumor, the CAR T cells, and the normal hematopoietic cells in the patient.

RESULTS

A total of 724 patients who had received T-cell therapies at our center were included in the study. A lethal T-cell lymphoma was identified in a patient who had received axicabtagene ciloleucel therapy for diffuse large B-cell lymphoma, and both lymphomas were deeply profiled. Each lymphoma had molecularly distinct immunophenotypes and genomic profiles, but both were positive for Epstein–Barr virus and were associated with *DNMT3A* and *TET2* mutant clonal hematopoiesis. No evidence of oncogenic retroviral integration was found with the use of multiple techniques.

CONCLUSIONS

Our results highlight the rarity of second tumors and provide a framework for defining clonal relationships and viral vector monitoring. (Funded by the National Cancer Institute and others.)

From the Divisions of Oncology (M.P.H., T.S., T.N., C.L.L., X.K., M.N.O., A.A.A.) and Blood and Marrow Transplantation and Cellular Therapy (M.P.H., S.D., M.J.F., D.B.M.), Department of Medicine, the Center for Cancer Cell Therapy (M.P.H., Z.G., S.D., M.J.F., B.S., C.L.M., D.B.M.), Stanford Cancer Institute (T.S., T.N., C.L.L., X.K., M.N.O., C.L.M., M.D., A.A.A., D.B.M.), the Department of Pathology (P.L.B., D.G.), the Department of Biomedical Data Science (Z.G.), the Division of Hematology and Oncology, Department of Pediatrics (C.L.M.), the Department of Radiation Oncology (M.D.), and the Institute for Stem Cell Biology and Regenerative Medicine (M.D., A.A.A.), School of Medicine, and the Department of Bioengineering, Schools of Medicine and Engineering (S.S.), Stanford University, Stanford, CA; and the Department of Pathology, Leiden University Medical Center, Leiden, the Netherlands (T.N.). Dr. Alizadeh can be contacted at arasha@stanford.edu or at Stanford University, SIM I Lokey Bldg., Rm. G2120B, Stanford, CA 94305.

Drs. Hamilton, Sugio, and Noordenbos and Drs. Alizadeh and Miklos contributed equally to this article.

N Engl J Med 2024;390:2047-60.
DOI: 10.1056/NEJMoa2401361

Despite the remarkable therapeutic efficacy of commercial chimeric antigen receptor (CAR) T-cell therapies,[1-9] concerns over toxicities remain. Recent reports described cases of postinfusion T-cell lymphoma after CAR T-cell therapy, which can be associated with integration of the CAR T-cell vector into the malignant lymphocytes.[10-15] These reports mirror previous concerns over vector integration causing direct tumorigenesis after gene therapy.[16-18]

The concern over vector integration leading to T-cell leukemia or lymphoma was highlighted by a recent Food and Drug Administration (FDA) announcement[19] that focused on gathering evidence of additional T-cell lymphomas after commercial CAR T-cell therapy, although the announcement also noted that the benefits of these therapies probably outweigh substantially the potential risks.[11] Since the release of this FDA alert describing 22 cases of T-cell lymphoma, with three of the lymphomas containing viral vectors, another CD8+ T-cell lymphoma was reported to harbor a *JAK3* lesion and was diagnosed approximately 3 months after commercial CD19-targeting CAR T-cell (CAR19) therapy.[10] The T-cell lymphoma clone was identified at low levels in the blood before the administration of CAR19 therapy, and vector levels in the clonal tissue were low. Accordingly, given the relatively small number of reported cases thus far, additional comprehensive genetic characterization of T-cell lymphomas after CAR T-cell therapy remains essential for understanding the risk of potential tumors with this therapy, as well as for defining the role of vector integration in malignant transformation.

We studied the incidence of a second tumor among 724 patients who had received infusions of adoptive cellular therapies at our institution and report a single case of an Epstein–Barr virus–positive (EBV+) T-cell lymphoma that was diagnosed 54 days after CAR T-cell therapy. We describe the molecular profile of this T-cell lymphoma and the antecedent diffuse large B-cell lymphoma (DLBCL) through deep molecular profiling, including flow cytometric immunophenotyping, targeted and whole-exome sequencing, and single-cell RNA and DNA sequencing of the incident T-cell lymphoma. We also describe profiling of serially collected plasma samples of cell-free DNA (cfDNA) for noninvasive genotyping, viral vector monitoring, and minimal residual disease assessment.

Methods

A detailed description of the methods for all the molecular techniques is available in the Supplementary Methods section in the Supplementary Appendix, available with the full text of this article at NEJM.org. These molecular techniques have also been described in previous studies.[20-23]

Case Report

Rarity of Secondary Cancers

We analyzed 791 therapeutic cell infusions in 724 unique patients at Stanford University Medical Center between February 4, 2016, and January 15, 2024 (Fig. 1A and Table S1 in the Supplementary Appendix). A total of 96.6% of the infusions were with CAR T cells, 0.8% were with cytokine-induced killer T cells, 1.5% were with cytotoxic T lymphocytes, and 1.1% were with specific peptide-enhanced affinity receptor T cells (hereafter referred to as CAR T-cell therapy). After a median follow-up of 15 months, we identified 25 second tumors, excluding nonmelanoma skin cancers. Of 14 hematologic second tumors, 13 were associated with myelodysplastic syndrome or acute myeloid leukemia and 1 was a T-cell lymphoma. Eleven second tumors were solid tumors (4 melanomas, 2 prostate carcinomas, 2 breast ductal carcinomas, 1 endometrial adenocarcinoma, 1 lung adenocarcinoma, and 1 metastatic mesothelioma) (Fig. S1A and S1B and Table S2). The cumulative incidence of a hematologic second tumor at 3 years was 6.5%, a finding that reflects the rarity of an incident second tumor after CAR T-cell therapy as previously reported.[15,24,25]

A Rare Case of T-Cell Lymphoma after CAR19 Therapy

The index T-cell lymphoma occurred in a 59-year-old woman who had received CAR19 therapy for stage IV EBV+ DLBCL that had originally manifested in the lymph nodes and bone marrow. Of note, the patient had a history of psoriasis and eosinophilic fasciitis, which had been treated with multiple agents over a 3-year period before the development of lymphoma (Fig. 1B and Fig. 2A). After early failures of frontline induction therapy

for the primary DLBCL and second-line chemoimmunotherapy regimens, the patient received CAR19 therapy with axicabtagene ciloleucel (axi-cel). Despite that a partial metabolic response was observed on day 28, clinically significant pancytopenia subsequently developed in the patient. On day 54, bone marrow biopsy revealed hemophagocytic lymphohistiocytosis associated with CD3+CD4+CD8–EBER+ T-cell lymphoma, with positron-emission tomography–computed tomography (PET-CT) confirming widespread nodal and marrow disease burden (Figs. 1B and 2A). After a substantial decline in the patient's performance status, she was unable to receive treatment for T-cell lymphoma and died of disease on day 62. Of note, the case in this index patient was among five cases of EBV+ DLBCL treated with axi-cel in our cohort; three other patients had disease progression by day 90 (two biopsy-proven relapses of DLBCL and one radiographic tumor progression at the original primary anatomical site), and one patient remained in remission after CAR19 therapy, despite the development of a secondary melanoma.

RESULTS

TUMOR PROFILING AND BLOOD MONITORING

To better understand any potential role for CAR19 vector integration in driving the index T-cell lymphoma, we performed comprehensive profiling of serially collected plasma samples from the patient (Fig. 1B and Table S3). Immunohistochemical features of the original DLBCL were consistent with an aggressive mature B-cell neoplasm with a nongerminal center B phenotype, expressing CD19, CD20, and EBV-encoded small RNA (EBER) in the atypical large B cells; there was no evidence of *MYC*, *BCL2*, or *BCL6* aberrations on fluorescence in situ hybridization. It is notable that at the time the DLBCL was diagnosed, no obvious morphologically abnormal T-cell population was observed, and the T cells were EBER– (Fig. 2A and Fig. S1C and Supplemental Note S1). In contrast, the subsequent EBV+ T-cell lymphoma was found to be CD3+CD4+CD8–EBER+, with no evidence of residual DLBCL according to morphologic or molecular criteria (Fig. 2A).

Minimal residual disease monitoring of the leukocytes from the peripheral blood and bone marrow, with the use of immunoglobulin-based high-throughput sequencing to track the DLBCL B-cell receptor immunoglobulin heavy-chain clonotype, revealed rapid eradication of B-cell lymphoma after axi-cel therapy (Fig. 2B). Similarly, using simultaneous tumor- and effector-cell profiling of cfDNA with CAPP-Seq (cancer personalized profiling by deep sequencing),[22] we again observed clearance of the previous B-cell lymphoma–derived circulating tumor DNA (ctDNA) (Fig. 2C). By means of T-cell receptor tracing, we found that the dominant TCRβ clonotype of the T-cell lymphoma identified in the day 54 bone marrow sample was also detectable before infusion in the day –88 lymph node and day –50 blood sample at low levels (0.006% and 0.0005% of cells, respectively [clonoSEQ assay, Adaptive Biotechnologies]) (Fig. 2B). This same TCRβ clonotype emerged on day 28 in the periphery and then dominated cfDNA by day 54 (Fig. 2C). Axi-cel expansion in the peripheral blood, as measured by flow cytometry (Fig. 2D and Fig. S2A), showed a normal peak[20] and remained at low levels until day 54. Coincident with development of the T-cell lymphoma clone and hemophagocytic lymphohistiocytosis, the plasma viral load for EBV also rose dramatically after CAR19 therapy (Fig. 2E).

SHARED AND DISTINCTIVE TUMOR MOLECULAR PROFILES

To better understand the clonal relationships between this T-cell lymphoma relative to the antecedent DLBCL, we performed comprehensive genetic profiling using CAPP-Seq and whole-exome sequencing of three preinfusion tumor samples, four serially collected plasma samples, and samples from the T-cell lymphoma itself (Fig. 1B, Fig. 2F). Gene expression profiles that were inferred noninvasively from the plasma samples with the use of EPIC-seq (epigenetic expression inference from cfDNA sequencing)[26] showed increased expression of several immune-cell and inflammatory markers alongside CD3 and CD4, a finding that is consistent with the origination of the T-cell lymphoma in the background of hemophagocytic lymphohistiocytosis (Fig. 2F ["gene expression"] and Fig. S2B). Molecular profiling of the DLBCL showed a mutation pattern consistent with previous EBV+ B-cell lymphoma[27,28] that was not detected in the T-cell

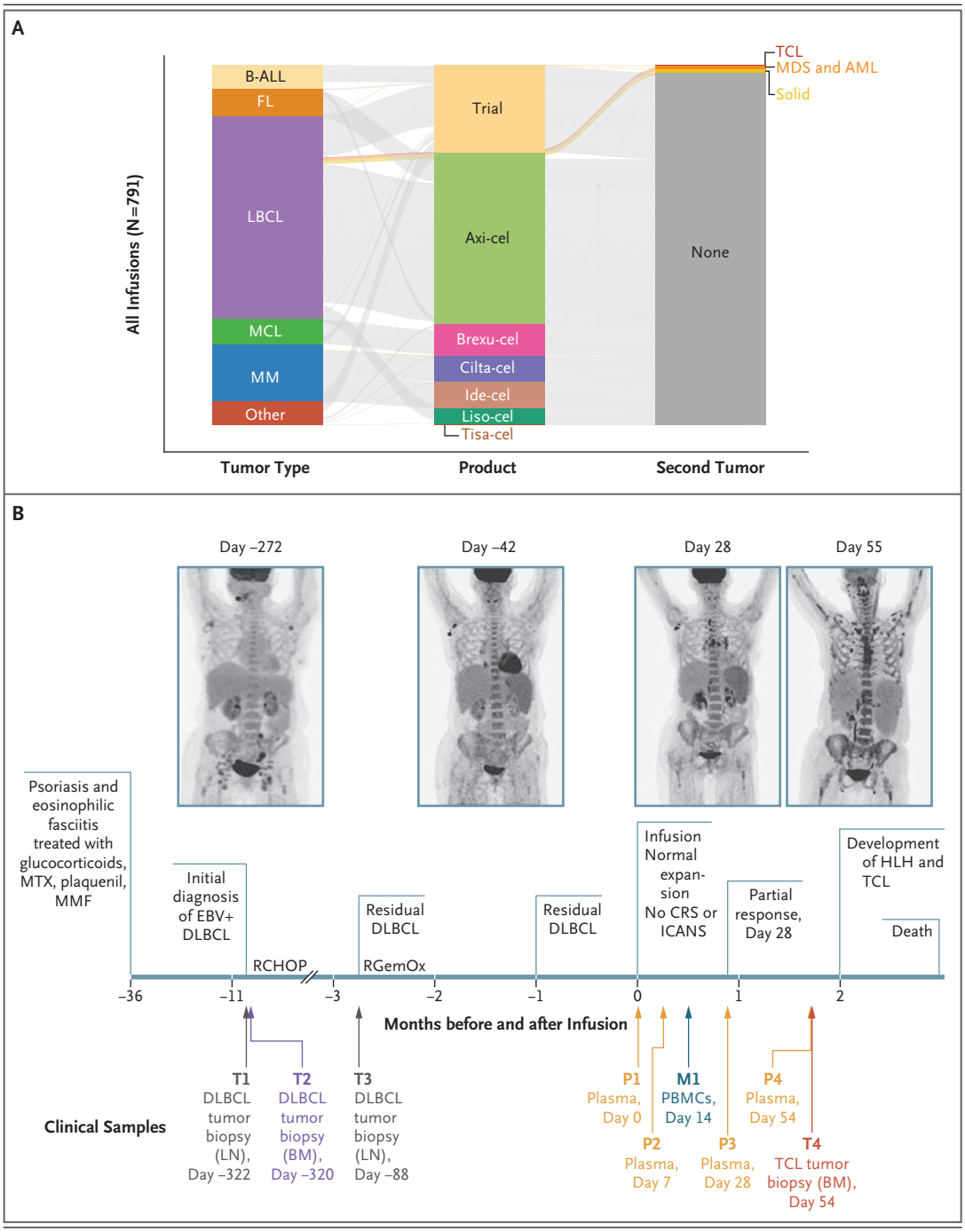

lymphoma sample (Fig. 2F ["DLBCL"]). Though the aggregate ctDNA minimal residual disease level was below the limit of detection, a single *CPEB2* mutation originally present in DLBCL tumors was also detected in the day 54 plasma sample; as such, small amounts of residual DLBCL or its progenitor clone could not be entirely ruled out. Conversely, the index T-cell lymphoma showed a mutational spectrum consistent with mature T-cell neoplasms, including an emergent FYN R176C-activating mutation that was not present in the original DLBCL

Figure 1 (facing page). Rarity of T-Cell Lymphoma Development after CD19-Targeting CAR T-Cell (CAR19) Therapy.

Panel A shows that among the patients who received chimeric antigen receptor (CAR) T-cell therapy at Stanford University (791 infusions in 724 patients), a single T-cell lymphoma (TCL) developed after standard care with axicabtagene ciloleucel (axi-cel) CAR19 infusion. Experimental products that were eventually approved for commercial distribution are included under their commercial name for the purpose of clarity. Lines between bar plots connect data for a single infusion. AML denotes acute myeloid leukemia, B-ALL B-cell acute lymphoblastic leukemia, brexu-cel brexucabtagene autoleucel, cilta-cel ciltacabtagene autoleucel, ide-cel idecabtagene vicleucel, FL follicular lymphoma, liso-cel lisocabtagene maraleucel, LBCL large B-cell lymphoma, MCL mantle-cell lymphoma, MDS myelodysplastic syndrome, MM multiple myeloma, and tisa-cel tisagenlecleucel. Panel B shows a timeline of the clinical course of disease and treatment in the index patient, a 59-year-old woman with an Epstein–Barr virus–positive (EBV+) diffuse large B-cell lymphoma (DLBCL) refractory to RCHOP (rituximab, cyclophosphamide, hydroxydaunorubicin [Adriamycin], oncovin–vincristine, and prednisone) and RGemOx (rituximab, gemcitabine, and oxaliplatin) chemotherapy. An EBV+ peripheral TCL–not otherwise specified developed subsequently (noted on day 54), leading to hemophagocytic lymphohistiocytosis and death. The major sequencing experiments that were performed in this study are shown along the timeline. T1, T2, and T3 indicate three preinfusion tumor samples; T4, the TCL sample drawn from a bone marrow biopsy; M1, peripheral-blood mononuclear cells (PBMCs); and P1, P2, P3, and P4, four serially collected plasma samples. BM denotes bone marrow, CRS cytokine-release syndrome, HLH hemophagocytic lymphohistiocytosis, ICANS immune effector cell–associated neurotoxicity syndrome, LN lymph node, MMF mycophenolate mofetil, and MTX methotrexate.

(Fig. 2F ["DLBCL" and "TCL"]). Both DLBCL and T-cell lymphoma tumor specimens contained mutations in *TET2* and *DNMT3A* at high variant allelic fractions, which suggests derivation from clonal hematopoiesis (Fig. 2F ["CH"]). The DLBCL tumor harbored a chr3q amplification and chr7 deletion, which were absent in the T-cell lymphoma, and the T-cell lymphoma harbored a chr1q amplification and chr6q deletion that were not detectable in the DLBCL tumor (Fig. 2F ["CNV"] and Fig. S2C). Collectively, these data suggest that although the DLBCL and T-cell lymphoma were molecularly distinct, the presence of shared lesions including mutations in *TET2* and *DNMT3A* implicate a common progenitor.

EVIDENCE AGAINST ONCOGENIC VECTOR EXPRESSION

To better define the phenotype of this post-CAR19 therapy T-cell lymphoma and assess it for the presence of the viral vector, we performed single-cell RNA profiling of bone marrow samples from the axi-cel–treated patient. For positive and negative controls, we used two axi-cel products that were created for infusion into different patients and bone marrow samples from five healthy controls, respectively (Fig. 3A and Fig. S3A and S3B). Within the bone marrow cells from the index lesion, we could readily identify a distinctive T-cell cluster that represented the malignant T cells (Fig. 3B and Fig. S3C). These T cells were highly clonal in consideration of the diversity at T-cell receptor loci (Fig. S3D) and had a CD3+CD4+CD8– phenotype, a finding consistent with the immunophenotype that was determined on histopathological analysis (Fig. S3E). The dominant TCRβ clone found in these single cells was indeed identical with that found in the plasma cfDNA by simultaneous tumor- and effector-cell profiling, as well as that found in the T-cell lymphoma tumor by T-cell receptor high-throughput sequencing (Fig. 2B and 2C and Fig. 3C).

Inferred copy-number profiles of the single cells within the malignant clone showed changes consistent with previously discovered structural rearrangements including 6q loss and 1q gain (Fig. 3D) and EBV positivity (Fig. 3E). The expressed gene program discovered in single-cell RNA sequencing included *BALF3-5*, *LF1-2*, and *BARF0*, which suggests an EBV-related lytic expression pattern.[29] A gene-expression profile in the tumor along with its mutation pattern and histopathological characteristics were most consistent with peripheral T-cell lymphoma–not otherwise specified (Fig. S3F).[30] Axi-cel vector transgene messenger RNA was conspicuously absent from the T-cell lymphoma tumor specimen (Fig. 3F), and the results of flow-cytometry profiling of the bone marrow specimen for surface CAR19 protein levels were consistent with this finding and did not show vector expression. Collectively, these data highlight the absence of evidence to directly implicate axi-cel vector activity at the RNA or protein level in this index T-cell lymphoma.

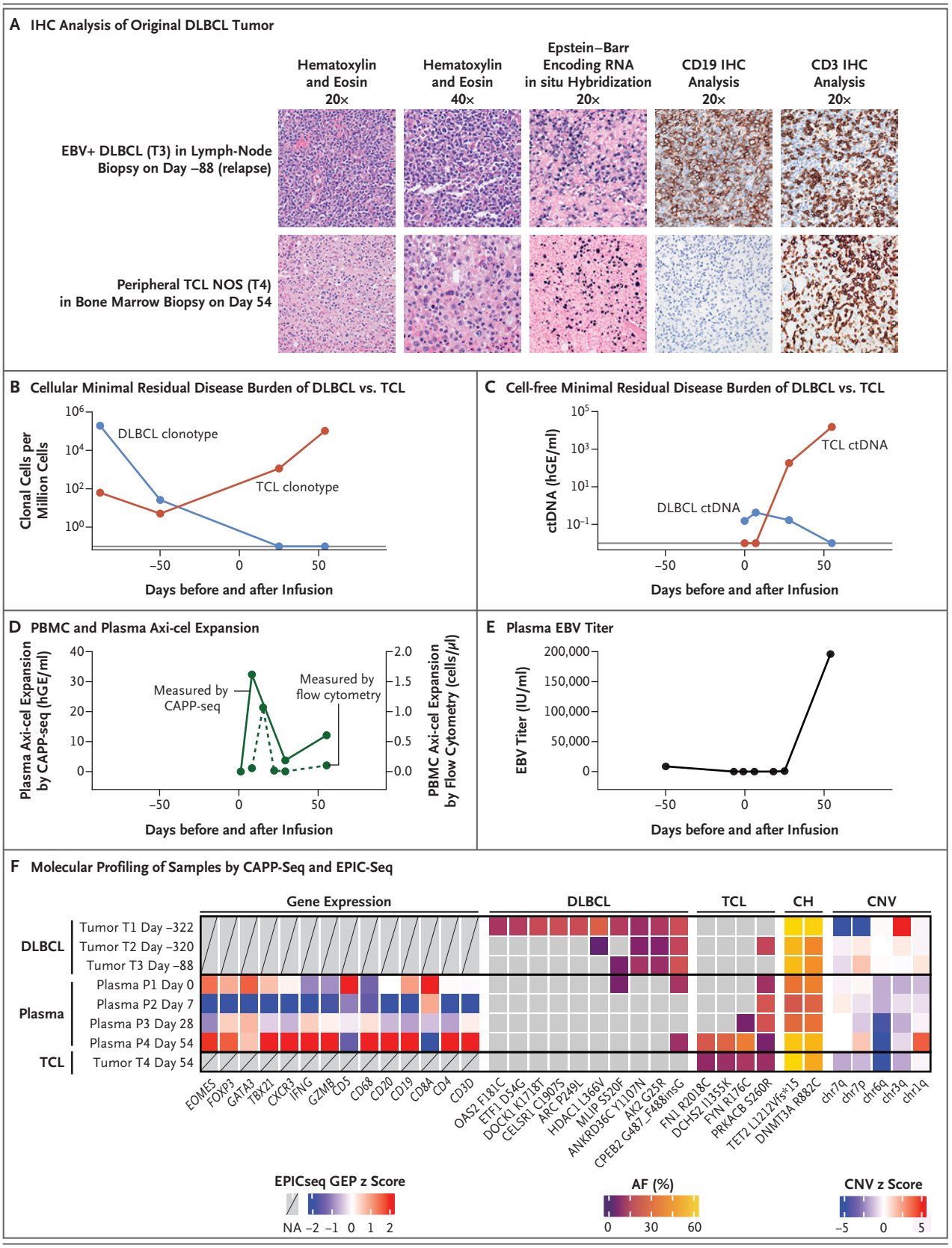

Figure 2 (facing page). Clinical and Molecular Characteristics of the Index TCL with Molecular Distinction from the DLBCL Clone.

Panel A shows the immunohistochemical (IHC) analyses of the original DLBCL tumor in the lymph node in which an abnormal population of large cells that were CD19+CD20+EBER+ was detected (top, CD20 staining not shown) and of the CD3+CD4+CD8−EBER+ index TCL (bottom, CD4 and CD8 staining not shown). NOS denotes not otherwise specified. Panel B shows the B-cell receptor clonotype analysis and the loss of DLBCL B-cell receptor detection after axi-cel infusion as measured by cellular profiling of the lymph nodes, blood, and bone marrow (clonoSEQ assay, Adaptive Biotechnologies). Longitudinal data points are depicted in the following order: DLBCL lymph node at day −88, peripheral blood at day −50, peripheral blood at day 25, and bone marrow harboring TCL. TCRβ tracing was performed by identifying the dominant clonotype in the index bone marrow specimen and determining clonal abundance in previous samples (P1 to P4) that were normalized as clones per million nucleated cells (see the Supplementary Methods in the Supplementary Appendix). The horizontal line at the bottom of the plot represents undetectable values. Panel C shows the CAPP-Seq (cancer personalized profiling by deep sequencing) profiling of the plasma samples. There was low-level detection of the original DLBCL at the time of axi-cel infusion, which subsequently became undetectable. At day 28, a novel TCR clone associated with the index TCL was detectable in the plasma by DNA capture profiling. This clone dominated circulation at the time the TCL became clinically apparent. The abbreviation ctDNA denotes circulating tumor DNA, and hGE haploid genome equivalents. The horizontal line at the bottom of the plot represents undetectable values. Panel D shows the axi-cel expansion and retraction as measured by hybridization capture sequencing (CAPP-Seq, solid line) on plasma samples and flow cytometry (dashed line) on PBMCs. Panel E shows that concurrent with development of the index TCL, EBV titers rose dramatically in the clinical profiling of the plasma samples. Panel F shows the comprehensive molecular profiling of serially collected samples by CAPP-Seq. The section of the grid labeled "gene expression" shows increased malignant TCR clonal load and increased EBV expression in conjunction with gain of CD3 and CD4 expression, as measured by epigenetic expression inference from cell-free DNA-sequencing (EPIC-seq). Gray boxes with a diagonal line indicate no data available. The grid sections labeled "DLBCL" and "TCL" show that the molecular mutational spectrum associated with the original DLBCL and the index TCL are distinct, thereby providing no evidence of transdifferentiation of the original DLBCL. Gray boxes indicate that the mutation is not detected. The grid section labeled "CH" (clonal hematopoiesis) shows the high burden of preexisting DNMT3A and TET2 clonal hematopoiesis, which was present at the time of diagnosis and remained at high levels throughout the patient's clinical course. The grid section labeled "CNV" (copy number variation) shows the copy number variation in the original DLBCL and the index TCL. DLBCL has a distinct chr3q gain and chr7 deletion, whereas the TCL has a distinct chr1q and chr6q loss. AF denotes allelic fraction, and GEP gene expression profiling.

EVIDENCE AGAINST ONCOGENIC VECTOR INTEGRATION

We next considered whether cryptic axi-cel integration into this T-cell lymphoma genome may not lead to axi-cel RNA or protein expression, yet nevertheless serve as an oncogenic event. As a first step to validate our single-cell RNA and protein-expression profiling results, we tested the index T-cell lymphoma for the presence of integrated vector DNA sequences by quantitative polymerase chain reaction. Although axi-cel was reliably detected in the day 14 control leukocytes as expected, it was not detected in bone marrow cells containing the T-cell lymphoma above the limit of detection of the assay (Fig. S4A).

We also considered whether cryptic retroviral integration and associated structural derangements may occur segmentally and thereby lead to fragments of the integrated axi-cel vector that may not be detectable with a single set of primers. To address this possibility, we first tested for evidence of axi-cel integration into the T-cell lymphoma genome using a 112-probe hybrid capture panel[22] consisting of overlapping 120-bp probes directed against the entire axi-cel retroviral vector. With this approach, the axi-cel vector was not detectable in the index T-cell lymphoma sample (a finding that was consistent with our previous results), despite having been reliably detected at day 7 and day 28 in plasma cfDNA and at day 14 in the circulating leukocytes during CAR19 expansion (Fig. 2D).

To test the presence of axi-cel DNA more definitively in the index lesion at single-cell resolution, we next targeted 11 tiled amplicons spanning the length of the integrated axi-cel vector (Fig. S4B). As positive controls, cytopenic bone marrow aspirates were obtained from seven unrelated patients who had received CAR19 therapy (date range of aspirates obtained after therapy, day 137 to day 1561). We reliably detected a low-level axi-cel signal in five of the seven controls at a frequency as low as 0.2% (range, 0.2 to 1.1) (Fig. S4C). Amplicon DNA content per cell correlated with paired RNA-sequencing data within the control samples (Fig. S4D). Concurrent cell-surface protein analysis with antibody probes showed that more than 93% of the axi-cel–positive

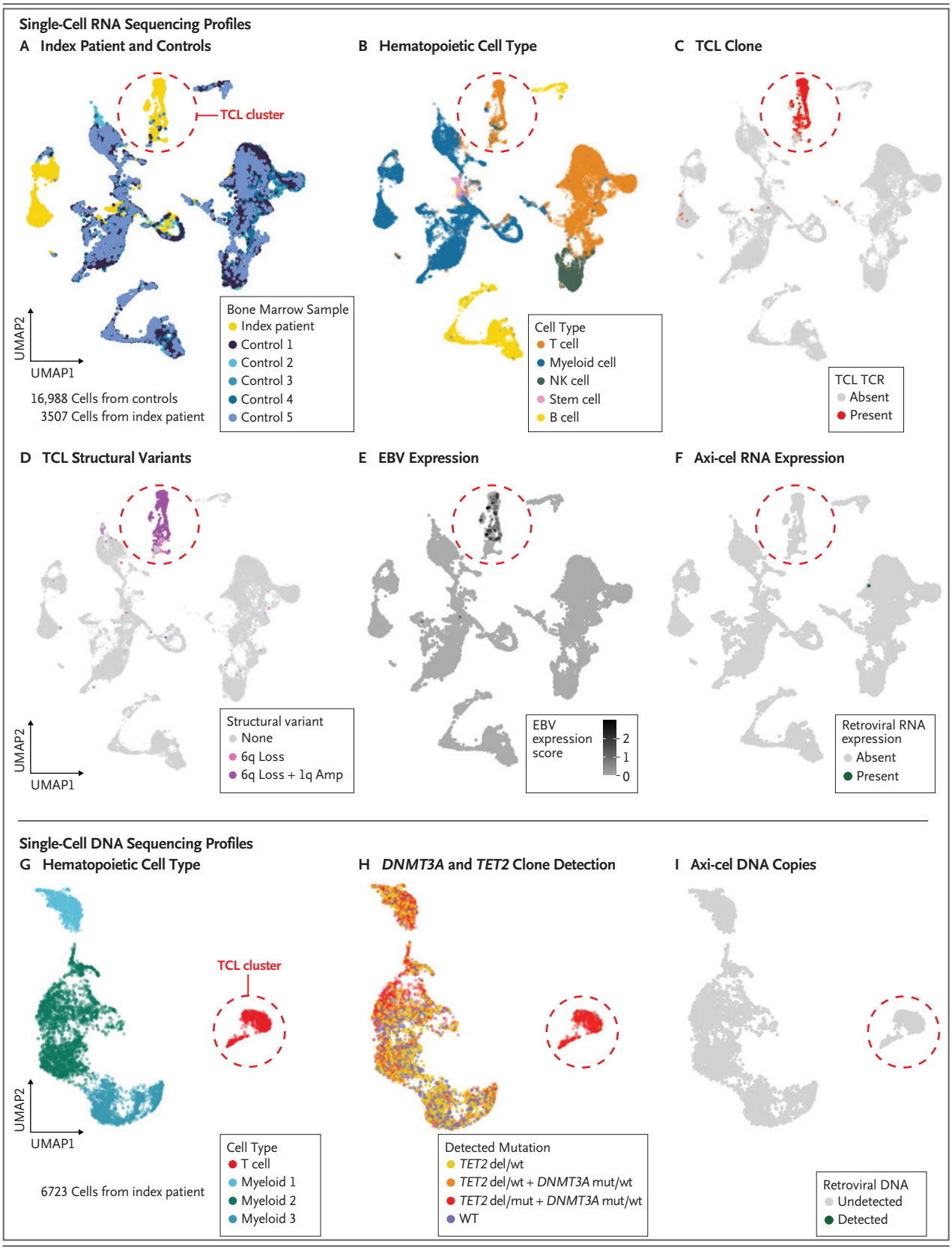

Figure 3 (facing page). Absence of Axi-cel Vector Integration on RNA and DNA Profiling of the Index TCL at Single-Cell Resolution.

Panel A shows the single-cell RNA analysis of the bone marrow sample from the index patient as compared with the bone marrow samples from five healthy controls. Distinct clustering of the pathologic marrow is shown to be consistent with the presence of TCL and hemophagocytic lymphohistiocytosis. Cells were plotted after dimensional reduction with the use of uniform manifold approximation and projection (UMAP). UMAP plots are a two-dimensional representation of high-level data. Single points represent single cells, and the distance between points represents similarity of the measured features (i.e., RNA or protein). Panel B shows cell-type prediction with the use of Seurat (a statistical package in R dedicated to the analysis of single-cell RNA data) and indicates that one of the index patient's unique clusters is defined as T cells. NK denotes natural killer. Panel C shows the single-cell T-cell receptor (TCR) sequencing, in which the previously described TCL clone that was identified in the plasma samples was found to match the T-cell cluster present in the index lesion. Panel D shows copy-number variation as determined by RNA inference, indicating that the novel T-cell cluster carries gain of chromosome 1q and loss of chromosome 6q consistent with DNA copy-number profiling. Panel E shows EBV RNA expression localizing to the putative malignant clone. Panel F shows the complete absence of axi-cel messenger RNA expression at single-cell resolution in the index TCL. Panel G shows that cell-surface antibody profiling combined with single-cell DNA profiling revealed a separate cluster containing primarily CD3+CD4+CD8– T cells consistent with the malignant clone. Panel H shows the single-cell DNA profiling of the preexisting DNMT3A R882C, *TET2* deletion, and TET2 L1212Vfs*15 clone. The same clonal hematopoiesis mutations were detected in the myeloid populations. "*TET2* del/wt" denotes *TET2* deletion only, "*TET2* del/wt+*DNMT3A* mut/wt" *TET2* deletion+DNMT3A R882C, "*TET2* del/mut+*DNMT3A* mut/wt" *TET2* deletion+DNMT3A R882C+TET2 L1212Vfs*15, and WT wild type. Panel I shows that single-cell DNA sequencing of axi-cel with the use of an 11-amplicon panel tiled across the axi-cel vector again failed to show any evidence of axi-cel integration into the index TCL. Red circles indicate the TCL cluster location in each UMAP plot.

cells were identified as T cells, thereby validating the sensitivity and specificity of the assay (Fig. S4E through S4H and Supplemental Note 2). The presence of axi-cel in nontransformed bone marrow specimens that were obtained up to 4 years after axi-cel treatment indicates the need for caution before assigning vector integration as a method of transformation. Indeed, persistence of CAR is expected at low levels for very prolonged periods after infusion.[31]

Having established the accuracy of this single-cell assay, we similarly characterized bone marrow containing the index T-cell lymphoma using our single-cell DNA panel with a total of 6723 cells assayed. Using multiplexed antibodies to barcode and index each single cell, we again identified a population of CD3+CD4+CD8– T cells that were consistent with the T-cell lymphoma, along with myeloid cell populations (Fig. 3G and Fig. S4I). It was notable that the preexisting heterozygous DNMT3A R882C and the TET2 L1212Vfs*15 clones were present in 97.9% of these T cells (Fig. 3H). This finding provides strong evidence for the T-cell lymphoma to be both DNMT3A R882C– and TET2 L1212Vfs*15–mutated and thus were probably derived from lymphoid clonal hematopoiesis present before infusion. The *TET2* clone was further characterized as hemizygous for L1212Vfs*15, which indicates a concurrent loss-of-heterozygosity event. Indeed, lineage-tracing analysis with copy-number-variation analysis in cells revealed a *TET2* deletion lacking DNMT3A R882C and TET2 L1212Vfs*15 in 31.5% of all cells (Fig. 3H), a finding that indicates *TET2* loss of heterozygosity to be the founding clonal event. After this event, the presence of a subset of *TET2*-deleted and *DNMT3A* mutant cells indicated DNMT3A R882C mutation to be a subsequent clonal event. Finally, the L1212Vfs*15 mutation was a third clonal event leading to the founder progenitor clone from which the malignant population was derived (Fig. S4J and S4K). The existence of the *DNMT3A* and *TET2* clones throughout the lymphoid and myeloid lineages in different proportions suggests that the original clone was derived from a hematopoietic stem or progenitor cell (*TET2* deletion+DNMT3A R882C+TET2 L1212Vfs*15 was found in 35.8% of the myeloid population).

Despite direct identification of the index lesion at single-cell resolution, axi-cel amplification across all 11 amplicons was conspicuously absent, thereby providing no evidence for fragmented DNA integration of the vector as a mechanism of tumorigenesis (Fig. 3I). Collectively, these results show the clear absence of evidence to directly implicate the viral vector in this T-cell lymphoma, as determined by multiple sensitive molecular assays to interrogate retroviral vector DNA, RNA, and protein at single-cell resolution.

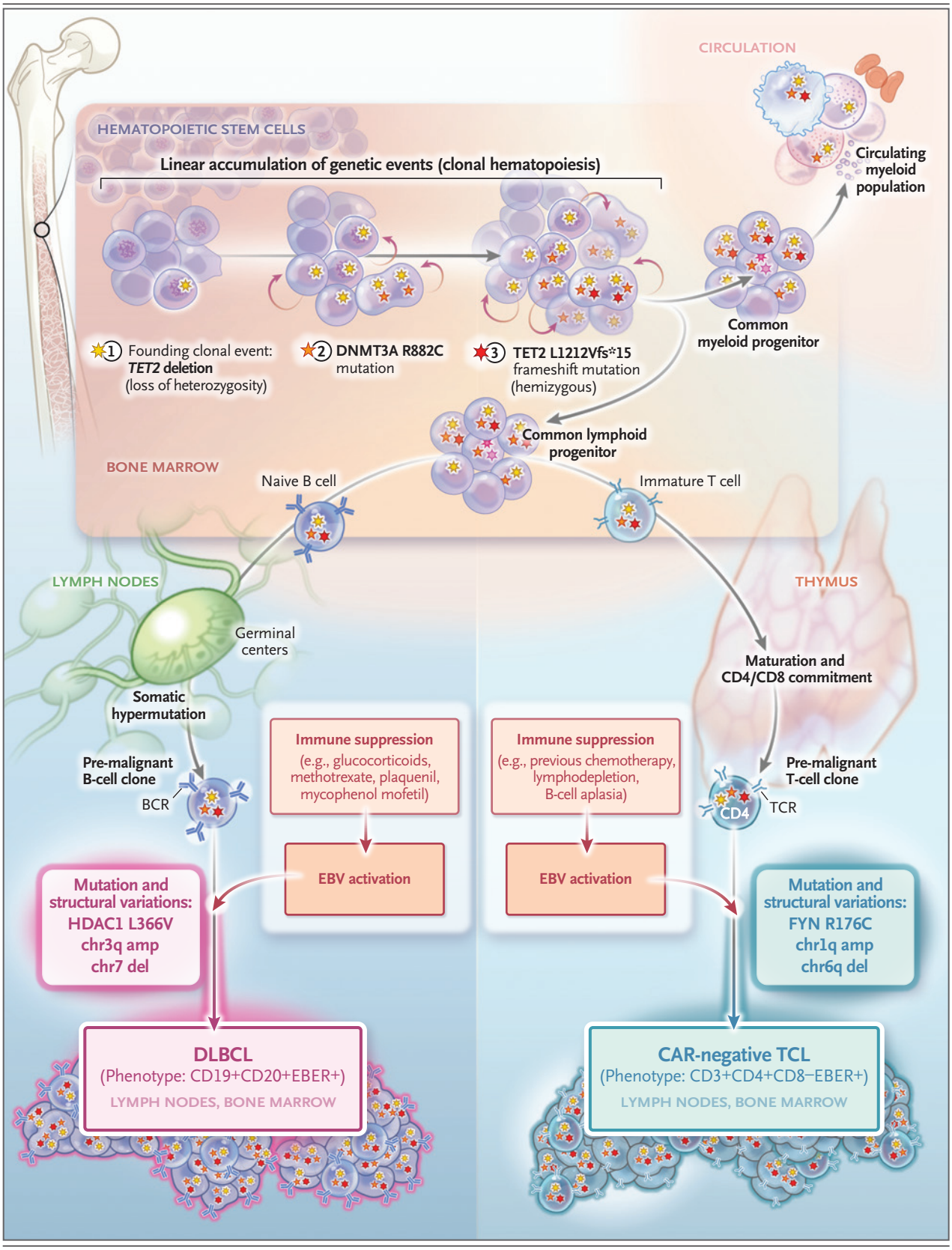

Figure 4 (facing page). Parallel Development of DLBCL and TCL from a Common Hematopoietic Progenitor-Cell Population.

Shown is a schematic of parallel development of DLBCL and TCL from a common hematopoietic progenitor-cell population. Single-cell DNA sequencing data indicate a linear accumulation of clonal hematopoiesis (*TET2* deletion→DNMT3A R882C mutation→TET2 L1212fs*15 mutation). The presence of this mutation in all cell populations in single-cell DNA sequencing data indicates that the founder population was in hematopoietic stem cells, which propagated into the common lymphoid progenitor and common myeloid progenitor. Both the DLBCL and TCL tumors contain recombined B-cell and T-cell receptors, respectively, a finding that is consistent with mature lymphoid neoplasms and that indicates that the DLBCL was derived after germinal center maturation and that the TCL was post-thymic. EBV activation due to immune suppression was probably a common event in both tumors but one that led to unique subsequent mutation and structural variation that resulted in the mature neoplasm. The malignant clones can be traced by their respective B-cell and T-cell receptor sequences and their unique mutational and structural changes.

DISCUSSION

Second neoplasms are now recognized as a risk after CAR19 therapy, with recent reports detailing higher odds ratio for myeloid and T-cell second tumors.[25] T-cell lymphomas are of particular interest in this clinical setting owing to the risk of CAR T-cell vector integration contributing to oncogenesis. This study describes comprehensive genomic profiling of a T-cell lymphoma arising after commercial CAR19 therapy at single-cell resolution (illustrated in Fig. 4). The methods used here serve as a resource and a benchmark for characterization of tumors after CAR T-cell therapy and for vector monitoring. After surveilling for second tumor in 724 patients who had received cellular therapy at our center, we found that T-cell lymphoma was rare, accounting only for a single case. No evidence was found to implicate a direct contribution from the engineered retroviral vector in the index T-cell lymphoma at the DNA, messenger RNA, or protein level and on interrogation of circulating, tissue-resident, and cell-free anatomical compartments. We found this index T-cell lymphoma to be molecularly distinct from the original DLBCL, with no evidence of lineage switch or transdifferentiation. Instead, the T-cell lymphoma clonotype was first detected before infusion of CAR T-cell therapy at day −88 and was associated with EBV+ lymphoproliferation, novel structural rearrangement, and a *FYN*-activating gene mutation. The preexisting clonal population retrospectively detected in the lymph nodes at day −88 was determined by TCRβ clonotype detection to be at a low level (0.006% of cells). Although we are unable to definitively establish whether this clone reflects a premalignant population or a mature, fully evolved neoplasm, the presence of this clone at detectable levels before infusion supports an underlying susceptibility preceding CAR T-cell therapy.

A bidirectional risk between B-cell lymphoma and T-cell lymphoma is known, with a standardized incidence of T-cell lymphoma after B-cell lymphoma that was described in a previous report to be approximately five times as high as that in the general population.[32] This higher incidence peaked in the first year after diagnosis, which possibly accounts for reports of T-cell lymphomas arising within 2 years after CAR T-cell therapy.[11] In this previous report,[32] among 288,478 patients with B-cell lymphoma, 354 T-cell lymphomas (0.12%) were observed to follow the B-cell lymphoma. Our observation of one T-cell lymphoma among 587 B-cell lymphomas (0.17%) is in line with these observations, but the analysis would benefit substantially from a pooled multiinstitutional analysis with confirmatory molecular testing for CAR T-cell vector insertion.

Supporting a priori susceptibility to T-cell lymphoma transformation, the presence of a preexisting heterozygous DNMT3A R882C and hemizygous TET2 L1212Vfs*15 comutant clone in the patient described in the current study suggests that underlying lymphoid clonal hematopoiesis was probably a modifying factor in this malignant condition, even if its presence alone is insufficient to drive the T-cell neoplasm. Given the underlying multilineage *DNMT3A* and *TET2* mutations,[33] we postulate that this tumor was derived from a *DNMT3A* and *TET2* comutant lymphoid progenitor. EBV tends to infect mature B cells, but it is also known to occasionally infect hematopoietic stem cells and progenitor cells. However, it is not possible to conclude at what level of differentiation EBV infection occurred in the present case (Fig. 4). This study highlights the critical potential of lymphoid clonal hematopoiesis mutations to transform into lymphoid malignant conditions as previously

reported[34] and further suggests preexisting susceptibility to T-cell lymphoma.[32] Such underlying *TET2* and *DNMT3A* mutations are known to drive both EBV+ DLBCL[28] and EBV+ T-cell lymphoma,[35] a fact that implicates a common lymphoid progenitor in the formation of both tumors. Given the prevalence of clonal hematopoiesis, screening patients for such mutations before CAR T-cell therapy may be infeasible, especially since the likelihood of curing aggressive lymphoma could outweigh the rare risk of transformation of preexisting clonal hematopoiesis mutations. In such patients, an alternative preemptive strategy to intercept second tumors after CAR T-cell therapies could involve more active noninvasive surveillance for both the dynamics of CAR T cells and clonal hematopoiesis under selection, by monitoring of cfDNA as described here. Caution is warranted if underlying susceptibility mutations are present during CAR T-cell therapy for nonmalignant conditions such as autoimmune disease, especially when other drivers of lymphoproliferation such as EBV are also present.

The tendency of TET2 or DNMT3A deficiency (but not both) to confer a selective fitness advantage for engineered T cells is well known from mouse models, especially in the CD8 lineage.[36-38] This effect is consistent with reports of long-lived CAR populations in human subjects after integration into *TET2* mutant lymphoid clonal hematopoiesis.[39] Nevertheless, in our index case, despite the high prevalence of comutant clonal hematopoiesis before CAR T-cell therapy posing a substantial risk for their transduction by the retroviral vector, CAR integration was not required for malignant transformation. Accordingly, this suggests that vector transduction is not necessary for malignant transformation of T-cells after CAR T-cell therapy. Additional work is needed to fully address the synergies between CAR therapies and clonal hematopoiesis, as relevant for T-cell lymphoma risk. This phenomenon may be more prominent with 4-1BB–containing vectors, which tend to have greater persistence over CD28 constructs. Of note, a recent report also identified a *TET2* mutant T-cell lymphoma after ciltacabtagene autoleucel infusion, with evidence of lentiviral integration.[13] These observations further reinforce the importance of characterizing lymphoid clonal hematopoiesis before and after CAR T-cell therapy.

Using multiple techniques, we found no evidence of axi-cel incorporation into this tumor. Our results are in contrast to rare previous reports of CAR vector integration into a second tumor from studies in which other therapeutic vectors including transposons were used.[13,14] Our findings are in line with a recent report of another post–CAR T-cell therapy T-cell lymphoma that similarly did not show CAR19 integration.[10] It is important to note that the lymphodepleting chemotherapy, CAR-mediated inflammation, and B-cell aplasia that are associated with immunosuppression may each have contributed to the EBV-driven lymphoproliferation for the case described here. Additional reports of EBV-driven T-cell lymphoma after CAR T-cell therapies would support this hypothesis. This type of immunosuppression is a key long-term toxicity associated with CAR19 therapy[40-42] and underlies nonrelapse mortality due to infection. Nevertheless, in our cohort, subsequent lymphoproliferative disorders did not develop in four additional patients with EBV+ DLBCL, and limited previous reports have suggested that CAR19 therapy can be safe in patients with EBV+ DLBCL.[43]

The findings from our study involving 724 patients expand on previous observations[10] to further suggest that the development of T-cell lymphoma after CAR T-cell therapy is rare and may occur through various mechanisms in susceptible patients. In our index case, despite comprehensive genetic profiling, we found no evidence for CAR T-cell vector integration into the T-cell lymphoma or evidence for CAR expression. Given the known increased baseline risk of second T-cell malignant tumors in patients with previous B-cell lymphomas even in the absence of CAR therapies,[32] the observed T-cell tumors after CAR T-cell therapies, in a sufficiently large population of patients, may reflect a bystander instead of a direct effect. In this context, emerging data suggest that an inflammatory memory characterizes a special subset of hematopoietic stem cells that expands with age and is enriched for somatic mutations associated with clonal hematopoiesis.[44] Although this remains to be definitively determined, we speculate that such mutant progenitors could be especially prone to

CAR-associated inflammation and corresponding selection pressures.

The content is solely the responsibility of the authors and does not necessarily represent the official views of the National Institutes of Health.

Supported by grants (NCI R01CA233975 and NCI P01 CA049605) from the National Cancer Institute, the Virginia and D.K. Ludwig Fund for Cancer Research, Kite-Gilead, and Adaptive Biotechnologies. Drs. Hamilton, Sugio, and Alizadeh are supported by the Leukemia and Lymphoma Society. Dr. Alizadeh is also supported by the Moghadam Family Professorship at Stanford University. Dr. Noordenbos is supported by a fellowship from the Lymph&Co Foundation and the European Union. Dr. Mackall is supported by the Parker Institute for Cancer Immunotherapy.

Disclosure forms provided by the authors are available with the full text of this article at NEJM.org.

We thank the Mission Bio support team for single-cell data analysis as well as the members of the Adaptive Biotechnologies team for their help in tumor receptor tracing. We thank the Stanford Correlative Science Unit including Zachary Ehlinger, Moksha Desai, Juancarlos Cancilla, and Shriya Syall for performing molecular assays.

REFERENCES

1. Neelapu SS, Locke FL, Bartlett NL, et al. Axicabtagene ciloleucel CAR T-cell therapy in refractory large B-cell lymphoma. N Engl J Med 2017;377:2531-44.
2. Locke FL, Miklos DB, Jacobson CA, et al. Axicabtagene ciloleucel as second-line therapy for large B-cell lymphoma. N Engl J Med 2022;386:640-54.
3. Schuster SJ, Bishop MR, Tam CS, et al. Tisagenlecleucel in adult relapsed or refractory diffuse large B-cell lymphoma. N Engl J Med 2019;380:45-56.
4. Bishop MR, Dickinson M, Purtill D, et al. Second-line tisagenlecleucel or standard care in aggressive B-cell lymphoma. N Engl J Med 2022;386:629-39.
5. Abramson JS, Palomba ML, Gordon LI, et al. Lisocabtagene maraleucel for patients with relapsed or refractory large B-cell lymphomas (TRANSCEND NHL 001): a multicentre seamless design study. Lancet 2020; 396:839-52.
6. Kamdar M, Solomon SR, Arnason J, et al. Lisocabtagene maraleucel versus standard of care with salvage chemotherapy followed by autologous stem cell transplantation as second-line treatment in patients with relapsed or refractory large B-cell lymphoma (TRANSFORM): results from an interim analysis of an open-label, randomised, phase 3 trial. Lancet 2022; 399:2294-308.
7. Berdeja JG, Madduri D, Usmani SZ, et al. Ciltacabtagene autoleucel, a B-cell maturation antigen-directed chimeric antigen receptor T-cell therapy in patients with relapsed or refractory multiple myeloma (CARTITUDE-1): a phase 1b/2 open-label study. Lancet 2021;398:314-24.
8. Rodriguez-Otero P, Ailawadhi S, Arnulf B, et al. Ide-cel or standard regimens in relapsed and refractory multiple myeloma. N Engl J Med 2023;388:1002-14.
9. Munshi NC, Anderson LD Jr, Shah N, et al. Idecabtagene vicleucel in relapsed and refractory multiple myeloma. N Engl J Med 2021;384:705-16.
10. Ghilardi G, Fraietta JA, Gerson JN, et al. T cell lymphoma and secondary primary malignancy risk after commercial CAR T cell therapy. Nat Med 2024;30: 984-9.
11. Verdun N, Marks P. Secondary cancers after chimeric antigen receptor T-cell therapy. N Engl J Med 2024;390:584-6.
12. Levine BL, Pasquini MC, Connolly JE, et al. Unanswered questions following reports of secondary malignancies after CAR-T cell therapy. Nat Med 2024;30:338-41.
13. Harrison SJ, Nguyen T, Rahman M, et al. CAR+ T-cell lymphoma post ciltacabtagene autoleucel therapy for relapsed refractory multiple myeloma. Blood 2023;142:Suppl 1:6939. abstract (https://ashpublications.org/blood/article/142/Supplement%201/6939/504399/CAR-T-Cell-Lymphoma-Post-Ciltacabtagene-Autoleucel).
14. Bishop DC, Clancy LE, Simms R, et al. Development of CAR T-cell lymphoma in 2 of 10 patients effectively treated with piggyBac-modified CD19 CAR T cells. Blood 2021;138:1504-9.
15. Steffin DHM, Muhsen IN, Hill LC, et al. Long-term follow-up for the development of subsequent malignancies in patients treated with genetically modified IECs. Blood 2022;140:16-24.
16. Hacein-Bey-Abina S, Von Kalle C, Schmidt M, et al. LMO2-associated clonal T cell proliferation in two patients after gene therapy for SCID-X1. Science 2003; 302:415-9.
17. Hacein-Bey-Abina S, von Kalle C, Schmidt M, et al. A serious adverse event after successful gene therapy for X-linked severe combined immunodeficiency. N Engl J Med 2003;348:255-6.
18. Hacein-Bey-Abina S, Garrigue A, Wang GP, et al. Insertional oncogenesis in 4 patients after retrovirus-mediated gene therapy of SCID-X1. J Clin Invest 2008;118: 3132-42.
19. Food and Drug Administration. FDA investigating serious risk of T-cell malignancy following BCMA-directed or CD19-directed autologous chimeric antigen receptor (CAR) T cell immunotherapies. November 28, 2023 (https://www.fda.gov/vaccines-blood-biologics/safety-availability-biologics/fda-investigating-serious-risk-t-cell-malignancy-following-bcma-directed-or-cd19-directed-autologous).
20. Hamilton MP, Craig E, Gentille Sanchez C, et al. CAR19 monitoring by peripheral blood immunophenotyping reveals histology-specific expansion and toxicity. Blood Adv 2024 March 18 (Epub ahead of print).
21. Good Z, Spiegel JY, Sahaf B, et al. Post-infusion CAR T_{Reg} cells identify patients resistant to CD19-CAR therapy. Nat Med 2022;28:1860-71.
22. Sworder BJ, Kurtz DM, Alig SK, et al. Determinants of resistance to engineered T cell therapies targeting CD19 in large B cell lymphomas. Cancer Cell 2023;41(1): 210-225.e5.
23. Alig SK, Shahrokh Esfahani M, Garofalo A, et al. Distinct hodgkin lymphoma subtypes defined by noninvasive genomic profiling. Nature 2024;625:778-87.
24. Hsieh EM, Myers RM, Yates B, et al. Low rate of subsequent malignant neoplasms after CD19 CAR T-cell therapy. Blood Adv 2022;6:5222-6.
25. Elsallab M, Ellithi M, Lunning MA, et al. Second primary malignancies after commercial CAR T-cell therapy: analysis of the FDA Adverse Events Reporting System. Blood 2024;143:2099-105.
26. Esfahani MS, Hamilton EG, Mehrmohamadi M, et al. Inferring gene expression from cell-free DNA fragmentation profiles. Nat Biotechnol 2022;40:585-97.
27. Frontzek F, Staiger AM, Wullenkord R, et al. Molecular profiling of EBV associated diffuse large B-cell lymphoma. Leukemia 2023;37:670-9.
28. Li Y, Xu-Monette ZY, Abramson J, et al. EBV-positive DLBCL frequently harbors somatic mutations associated with clonal hematopoiesis of indeterminate potential. Blood Adv 2023;7:1308-11.
29. Yap LF, Wong AKC, Paterson IC, Young LS. Functional implications of Epstein-Barr virus lytic genes in carcinogenesis. Cancers (Basel) 2022;14:5780.
30. Iqbal J, Wright G, Wang C, et al. Gene expression signatures delineate biological and prognostic subgroups in peripheral T-cell lymphoma. Blood 2014;123:2915-23.
31. Melenhorst JJ, Chen GM, Wang M, et al. Decade-long leukaemia remissions with persistence of $CD4^+$ CAR T cells. Nature 2022;602:503-9.

32. Chihara D, Dores GM, Flowers CR, Morton LM. The bidirectional increased risk of B-cell lymphoma and T-cell lymphoma. Blood 2021;138:785-9.
33. Wang J, Su M, Wei N, et al. Chronic active Epstein–Barr virus disease originates from infected hematopoietic stem cells. Blood 2024;143:32-41.
34. Niroula A, Sekar A, Murakami MA, et al. Distinction of lymphoid and myeloid clonal hematopoiesis. Nat Med 2021;27:1921-7.
35. Kato S, Hamada M, Okamoto A, et al. EBV+ nodal T/NK-cell lymphoma associated with clonal hematopoiesis and structural variations of the viral genome. Blood Adv 2024;8:2138-47.
36. Prinzing B, Zebley CC, Petersen CT, et al. Deleting DNMT3A in CAR T cells prevents exhaustion and enhances antitumor activity. Sci Transl Med 2021;13(620):eabh0272.
37. Belizaire R, Wong WJ, Robinette ML, Ebert BL. Clonal haematopoiesis and dysregulation of the immune system. Nat Rev Immunol 2023;23:595-610.
38. Jain N, Zhao Z, Feucht J, et al. TET2 guards against unchecked BATF3-induced CAR T cell expansion. Nature 2023;615:315-22.
39. Fraietta JA, Nobles CL, Sammons MA, et al. Disruption of TET2 promotes the therapeutic efficacy of CD19-targeted T cells. Nature 2018;558:307-12.
40. Baird JH, Epstein DJ, Tamaresis JS, et al. Immune reconstitution and infectious complications following axicabtagene ciloleucel therapy for large B-cell lymphoma. Blood Adv 2021;5:143-55.
41. Hamilton MP, Miklos DB. Chimeric antigen receptor T-cell therapy in aggressive B-cell lymphoma. Hematol Oncol Clin North Am 2023;37:1053-75.
42. Rejeski K, Perez A, Sesques P, et al. CAR-HEMATOTOX: a model for CAR T-cell-related hematologic toxicity in relapsed/refractory large B-cell lymphoma. Blood 2021;138:2499-513.
43. Nair R, Ayers A, Nastoupil LJ, et al. CD19 CAR-T outcomes in patients with EBV-positive DLBCL. Blood 2022;140:Suppl 1:3800-2. abstract (https://ashpublications.org/blood/article/140/Supplement%201/3800/489877/CD19-CAR-T-Outcomes-in-Patients-with-EBV-Positive).
44. Jakobsen NA, Turkalj S, Zeng AGX, et al. Selective advantage of mutant stem cells in clonal hematopoiesis occurs by attenuating the deleterious effects of inflammation and aging. September 14, 2023 (https://www.biorxiv.org/content/10.1101/2023.09.12.557322v1) (preprint).